Journal of Oceanology and Limnology
Vol. 44, No. 3, pp. 990-1004, 2026
https://doi.org/10.1007/s00343-025-5062-8

Research Paper

Oceanographic significance of planktonic foraminiferal assemblages in the northwest Indian Ocean-Basin-Ridge system under monsoon influence*

Feng WANG[1], Yunhai LI[1, 2, **], Xuan DING[3], Mingjiang CAI[4], Zhikun LAI[1], Jian CHEN[1], Pengfei SHEN[5], Liang WANG[1], Xiang YE[1]

[1] *Third Institute of Oceanography, Ministry of Natural Resources, Xiamen 361005, China*
[2] *Laboratory for Marine Geology, Qingdao Marine Science and Technology Center, Qingdao 266237, China*
[3] *Oceanography Institute, China University of Geosciences (Beijing), Beijing 100083, China*
[4] *School of Resources and Environmental Science, Quanzhou Normal University, Quanzhou 362000, China*
[5] *Beijing Institute of Geothermal Research, Beijing 100012, China*

Received Mar. 3, 2025; accepted in principle Jun. 17, 2025; accepted for publication Aug. 20, 2025

Abstract Planktonic foraminifera in ocean sediments serve as unique paleoenvironmental recorders, and their distribution and diversity are affected by environmental factors. The northwest Indian Ocean, influenced by monsoons and ocean-basin-ridge systems, is a key research area in this regard. However, few studies have focused on the foraminiferal distribution in surface sediments. We analyzed 60 surface sediment samples in April 2023, from which 11 genera and 32 warm-water species were identified. The distribution was primarily controlled by depth-dependent carbonate dissolution, temperature-salinity gradients, and monsoon-driven hydrography. Four distinct assemblages were identified: the Arabian Basin assemblage (dominated by *Globorotalia cultrata*) demonstrates strong influence from the Arabian Sea high-salinity water and winter monsoon circulation; the Carlsberg Ridge assemblage (dominated by *G. cultrata*, *Globorotalia tumida*) exhibits depth-controlled productivity signatures; the Carlsberg Ridge Flanks assemblage (mainly including *Globigerinita glutinata*, *G. cultrata*, *Globigerinoides ruber*) reflects monsoon-induced mixing processes; and the Somali Basin assemblage (including mainly *G. cultrata*, *Pulleniatina obliquiloculata*, *G. tumida*) shows clear imprints of summer monsoon upwelling. Carbonate dissolution in the Somali Basin is strongest, followed by Arabian Basin, the Carlsberg Ridge showed the weakest dissolution. Based on planktonic foraminiferal abundance, fragmentation rate, $CaCO_3$ content, and dissolution susceptible/resistant species, the carbonate lysocline and compensation depth were estimated at ~3 700 and ~4 800 m, respectively.

Keyword: northwest Indian Ocean; surface sediment; planktonic foraminifera assemblage

1 INTRODUCTION

The northwest Indian Ocean is a distinctive region directly influenced by the monsoonal climatic and oceanographic conditions of the area, including the Arabian Sea, the Somali Sea, and the Carlsberg Ridge. Under the influence of monsoons, different sedimentary systems are formed, and environmental factors such as salinity, temperature, the direction of ocean current migration, and nutrient salts in different geomorphic units constitute sedimentary systems with regional characteristics (Banerjee and Iye, 1991; Schott and McCreary, 2001; Jin, 2004; Liu et al., 2022). Planktonic foraminifera are a significant component of the marine organisms and are an important issue of marine geological study. Their distribution and assemblages are key evidence for the evolution of marine environments. The investigation of distribution

* Supported by the National Program on Global Change and Air-Sea Interaction (Nos. GASI-04-HYDZ-02, GASI-01-WIND-CJ08, GASI-01-WIND-CJ09) and the National Natural Science Foundation of China (No. 42406074)

** Corresponding author: liyunhai@tio.org.cn

patterns of major foraminiferal genera under diverse marine environmental conditions is of great significance in comprehending past and future paleoenvironments and paleoceanography. These assemblages of planktonic foraminifera indicate specific ecological environments, reflecting environmental characteristics like water mass distribution, ocean current conditions, climate change, and biological effects (Illing, 1950; Wang et al., 1988a, b; Banakar et al., 2010; Ravichandran et al., 2021).

Foraminifera have been used in previous studies to make notable contributions to paleoceanography in the northwest Indian Ocean, specifically in relation to long and short-scale changes in the Indian monsoon and thermocline changes (Banakar et al., 2010; Arumugm et al., 2014; Cariño et al., 2023), changes in ancient marine environments (Hermelin, 1992; Rai and Srinivasan, 1994; Ciarapica, 1995; Gupta, 1997; Gupta and Thomas, 1999; Arumugm et al., 2014). Many reports on planktic foraminifera from the Arabian Sea are available (Bé et al., 1971; Brummer and Geert, 2002). These reports mainly focus on the coastal zone near the Arabian Sea, the Somali Basin, or the Carlsberg Ridge, but lack comparative connections among different geomorphic units. We documented the distribution of planktic foraminifera in the northwest Indian Ocean area, including the Carlsberg Ridge area, the Somali Basin, and the Arabian Basin (Barber et al., 2001; Gischler et al., 2003, 2008; Gupt et al., 2006; Boudagher-Fadel, 2008).

Our aim was to reveal the composition of planktonic foraminifera in various marine environments and their distribution in the region in relation to monsoon effects. Ultimately, we hope that our work could lay the foundation for future research into the case in the Indian Ocean. Meanwhile, this study can serve as a corrective approach for interpreting the core records of paleoceanographic changes and unveiling the past monsoon variability from sedimentary archives.

2 REGIONAL SETTING

2.1 Bathymetry

The study area in the northwest Indian Ocean encompasses the Carlsberg Ridge, with the Arabian in the north and the Somali Sea in the south. It spans 50°E–65°E and 0°–20°S, including the hydrothermal field of the Carlsberg Ridge, which is bordered by the Arabian Basin to the north and the Somali Basin to the south. The sampling was carried out at depths from 2 800 to 5 085 m (Ray et al., 2012) (Fig.1).

2.2 Surface current

Surface currents in the northern Indian Ocean are dominated by the tropical monsoon. During the October to March–April, a strong high-pressure system covered the Asian continent, resulting in the prevalence of the northeast monsoon over the northern Indian Ocean. The sea water in the Bay of Bengal flowed to the southwest and surrounds the island of Sri Lanka in the south, and mixed with the seawater flowing to the southwest of the Arabian Sea, forming the northeast monsoon current (NMC) and west Indian coastal current (WICC). Subsequently, the current flows south along the coast of the Somali Peninsula, forming the Somali Current, and converged with the Northern Equatorial warm current. From the May to September, the southwest monsoon prevailed, resulting in the seawater movement roughly opposite to that in winter, flowing east or northeast. The northern branch of the Southern Equatorial warm current crossed the equator under the influence of the monsoon, entered the northern Indian Ocean, flowed northeast along the coast of Somalia. A Somali current was formed. Upwelling in the northwest Indian Ocean was confined to the coastal zone east of the Somalia and Arabian, forming Arabian Sea high-salinity water (ASHSW) in the Arabian Basin (Banerjee and Iyer, 1991; Kroon et al., 1991; Chen et al., 1994; Prasad et al., 2001; Peng et al., 2015; Rippert et al., 2015).

According to their characteristics, ocean currents can be classified into warm currents and cold currents. In general, the monsoon current in the north Indian Ocean is considered a warm current throughout the year due to its location in the tropics and the high sea surface temperature (SST). This is attributed to the equatorial current, which is also a warm current. However, the ocean currents off the coast of Somalia exhibit an exception to this pattern (Rao and Sivakumar, 1998). During winter, a warm Somali Current is observed, while a Somali Current (cold) is observed during summer. This phenomenon is caused by the prevalence of southwest wind in the coastal waters of the Somali Peninsula during summer, which blows the surface seawater away from the coast, causing the deep seawater to rise due to compensation, forming a strong upwelling, and a significant drop in water temperature. Consequently, the ocean current in this region becomes a cold current (Quadfasel and Schott, 1982; You, 1997; Dahl and Oppo, 2006; Pandey et al., 2015).

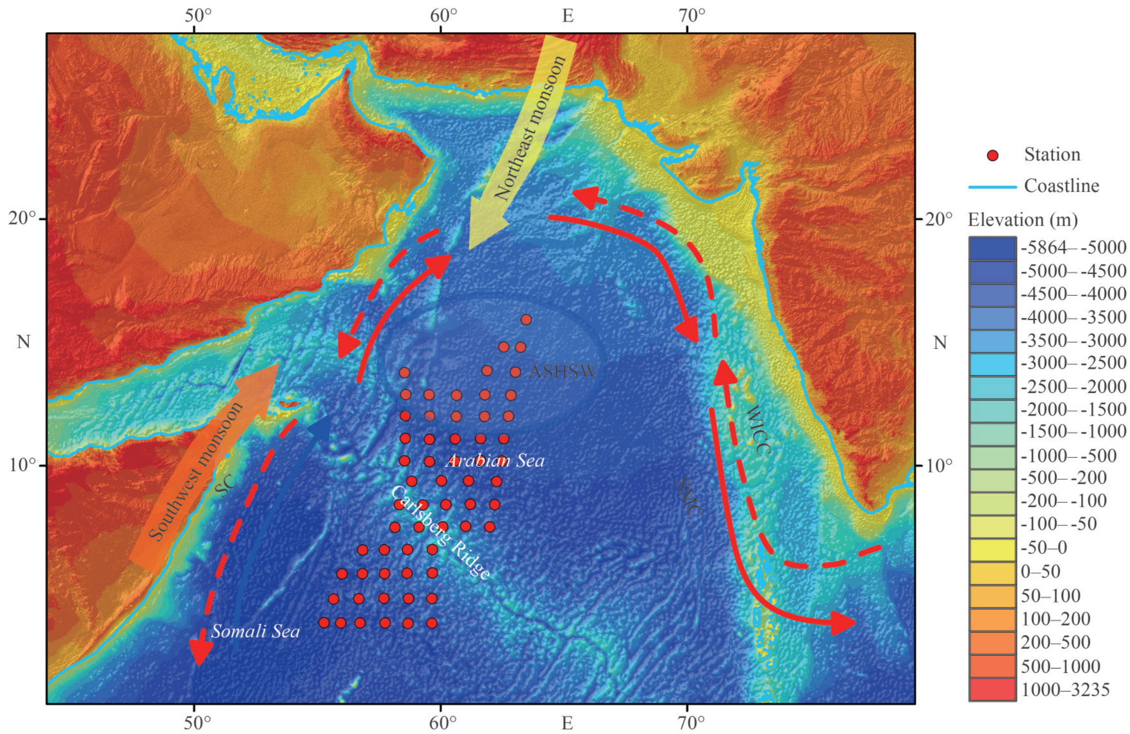

Fig.1 Station location (red dots) and surface circulation of the study area

The surface circulations in the Arabian Sea and Somali Sea in the summer and winter (dashed) are indicated. Red represents warm current, and blue for cold current. SC: Somali Current; WICC: west Indian coastal current; SMC: summer monsoon current; ASHSW: Arabian Sea high-salinity water. The summer and winter monsoon data are based on the World Ocean Atlas (WOA).

2.3 Distribution of water temperature and salinity

The surface sea temperature in the survey area ranges from 27 to 28 °C. There is a gradual increase in surface sea temperature from the western coastal zone towards the east. At a depth of 50 m, the seawater temperature varies between 24.5 and 26.5 °C, following a similar trend to that observed at the surface. The temperature distribution is centered mainly around the Somali Basin and the Arabian Basin, with temperatures decreasing radially outward. At 120 m, the central temperature of both basins is 21.4 °C, while at 200 m it drops to 15.6 °C. Surrounding areas at these depths exhibit temperatures approximately 1 °C lower (Fig.2).

Regarding salinity, sea surface salinity (SSS) increases from south to north, ranging from 35 to 38.2. Notably, within the ASHSW at a depth of 100 m, the temperature ranges from 24 to 28 °C and the salinity from 35.3 to 36.7 (Fig.3).

3 MATERIAL AND METHOD

3.1 Material

The 60 surface samples were obtained by a box-corer using R/V "*Xiangyang Hong 03*", and the sediments are mainly calcareous ooze, and a small number of stations are calcareous clay.

3.2 Identification of foraminifera

Prior to conducting the foraminifera analysis, the samples were dried at 60 °C and then soaked in clean tap water for 24 h for full dispersion. The soaked samples were repeatedly rinsed using a 63-μm size sieve. After rinsing, the samples were dried at 60 °C. Finally, dried foraminifera of the >150-μm size fraction were identified and counted under an Olympus SZX16 microscope (Kennett, 1983; Darling et al., 2006; Spezzaferri et al., 2015; Brummer and Kučera, 2022).

Fragment %=(number of fragments/8)/((number of fragments/8)+(complete number of planktonic foraminifera))×100 (Le and Shackleton, 1992).

3.3 Calcium carbonate content

The sample was first freeze-dried for 12 h, and then dried in oven at 60 °C for at least 6 h. 50 mg of the processed sample was weighed and placed in a tinfoil cup for total carbon (TC) content analysis using an elemental analyzer (Vario EL III Elemental

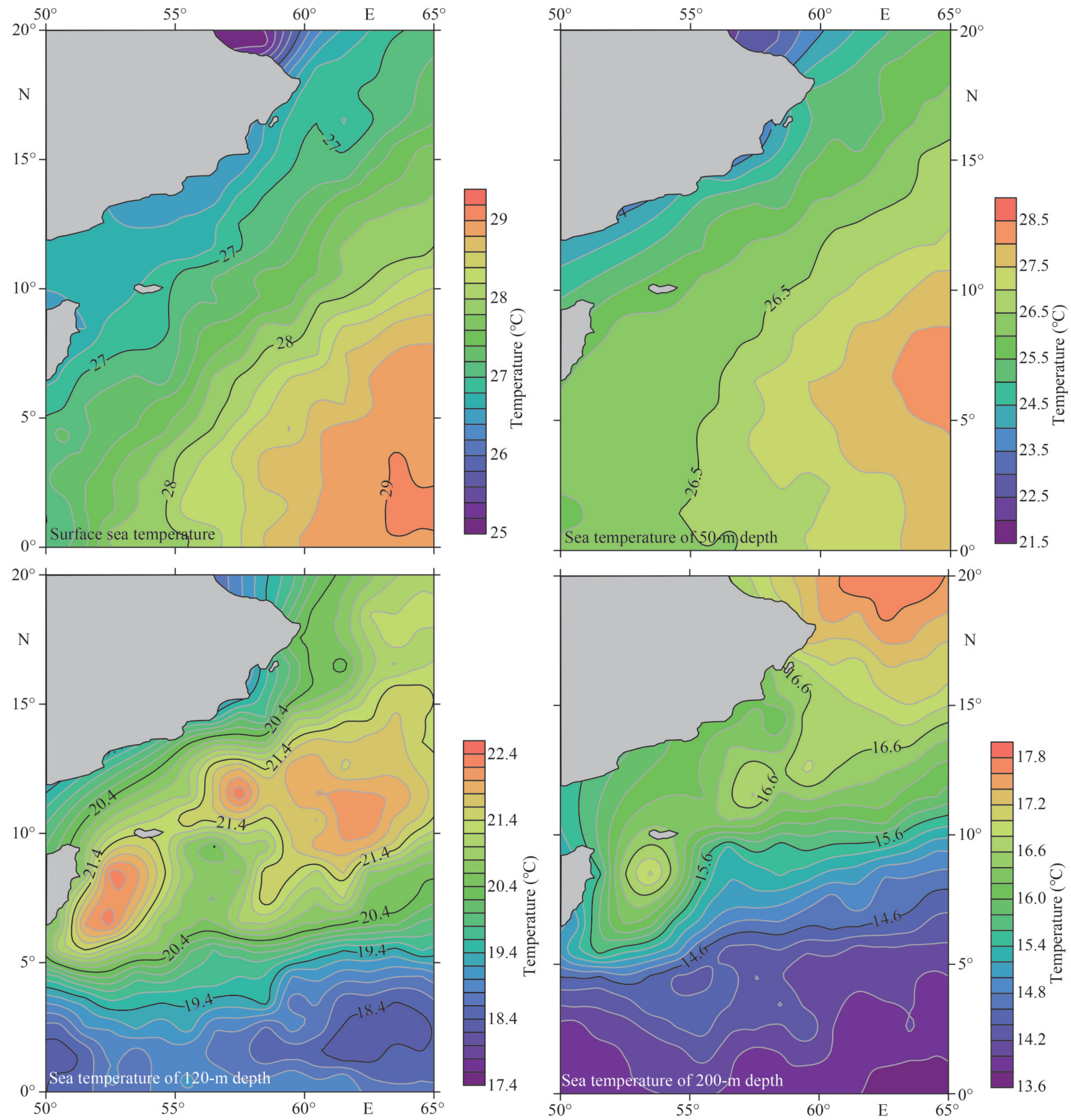

Fig.2 Water temperature in the northwest Indian Ocean

Data source: https://www.nodc.noaa.gov.

Analyzer). For organic carbon (OC) analysis, 1 g of the lyophilized and fully ground sediment sample was weighed, mixed with 2 mL of 1-mol/L dilute hydrochloric acid, sonicated for about 3 h, and then heated on a low-temperature electric heating plate for about 12 h. After HCl volatilized, the difference between the total carbon and organic carbon was calculated as inorganic carbon (IC). Standard sample (GSD-9) was used to test the parallel standard samples. The absolute error of three repeated determinations of the element standard samples was less than ±0.3%, and the difference between the analysis results of each element parallel sample was less than 0.6%.

The content of calcium carbonate was calculated based on the content of TC and TOC, using the following formula:

$$CaCO_3=(TC-TOC)\times 8.33\%.$$

4 RESULT

The samples in the study area were dominated by planktonic foraminifera, including 11 genera and 32

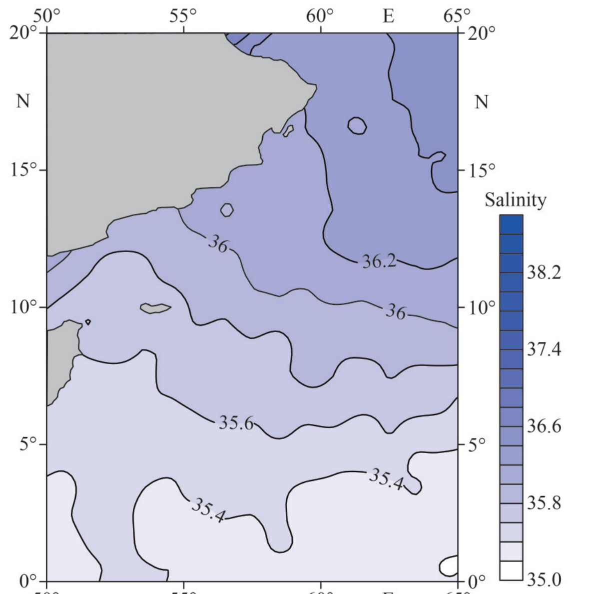

Fig.3 Sea surface salinity distribution map of seawater in the investigation area

Data from https://www.nodc.noaa.gov.

species identified, and a small amount of benthic foraminifera. The overall appearance was typical of tropical and subtropical regions. The abundance of planktonic foraminifera ranged from 0 to 26 130/g, with the highest values observed in the Carlsberg Ridge area (8 000–26 130/g). The abundance of planktonic foraminifera in the Arabian Basin was slightly greater than that in the Somali Basin, but both were below 4 000/g. The high-value area of composite divergence of planktonic foraminifera was also observed in the Carlsberg Ridge area (average 1.93), followed by the Somali Basin (average 1.46), and the lowest composite divergence in the Arabian Basin (average 1.16). The planktonic foraminifera fragment rate between 2.72%–86.90%, with an average of 48.69%. The Somali Basin has the highest fragmentation rate (average 63.28%), followed by the Arabian Basin (average 58.13%), and the Carlsberg Ridge has the lowest (average 35.86%). Therefore, we inferred that carbonate dissolution is the strongest in the Somali Basin, followed by the Arabian Basin, and the weakest in the Carlsberg Ridge (Fig.4).

The dominant species having average content of >5% in the planktonic foraminifera assemblage included *Globigerinita glutinata*, *Globorotalia cultrata* (Brummer and Kučera, 2022), *Globorotalia tumida*, *Pulleniatina obliquiloculata*; those of 3%–5% included *Globigerinoides ruber*, *Trilobatus trilobus* (Spezzaferri et al., 2015), *Neogloboquadrina dutertrei*; and the rest included *Globigerina bulloides*, *Globigerinella calida*, *Globigerinoides conglobatus*, *Neogloboquadrina incompta* (Darling et al., 2006), *Sphaeroidinella dehiscens*, etc. These genera and species are common in the tropical-subtropical water masses (Fig.5).

4.1 Distribution of dominant species

The planktonic foraminifera species and their assemblages reflect environmental characteristics of different sea areas. The distribution traits of main species (Fig.6) are as follows:

Globorotalia cultrata is the most abundant, a large-shelled dissolution-resistant species indicating upwelling (Bé and Hutson, 1977; Berger, 1979; Chen et al., 1991; Chen et al., 1999). It dominates northern Arabian Sea Basin (over 90%), with lower abundances in the south (25% in Carlsberg Ridge ~40% in Somali Basin). Its 79.18% abundance in Arabian Basin correlates with ASHSW from winter

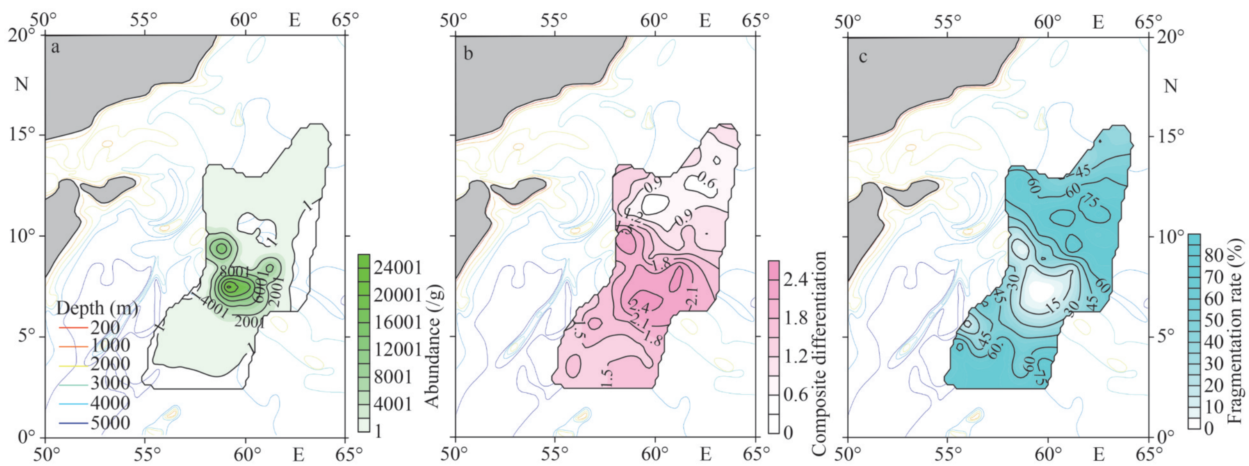

Fig.4 The abundance (a), the composite differentiation (b), and the fragmentation rate (c) of planktonic foraminifera

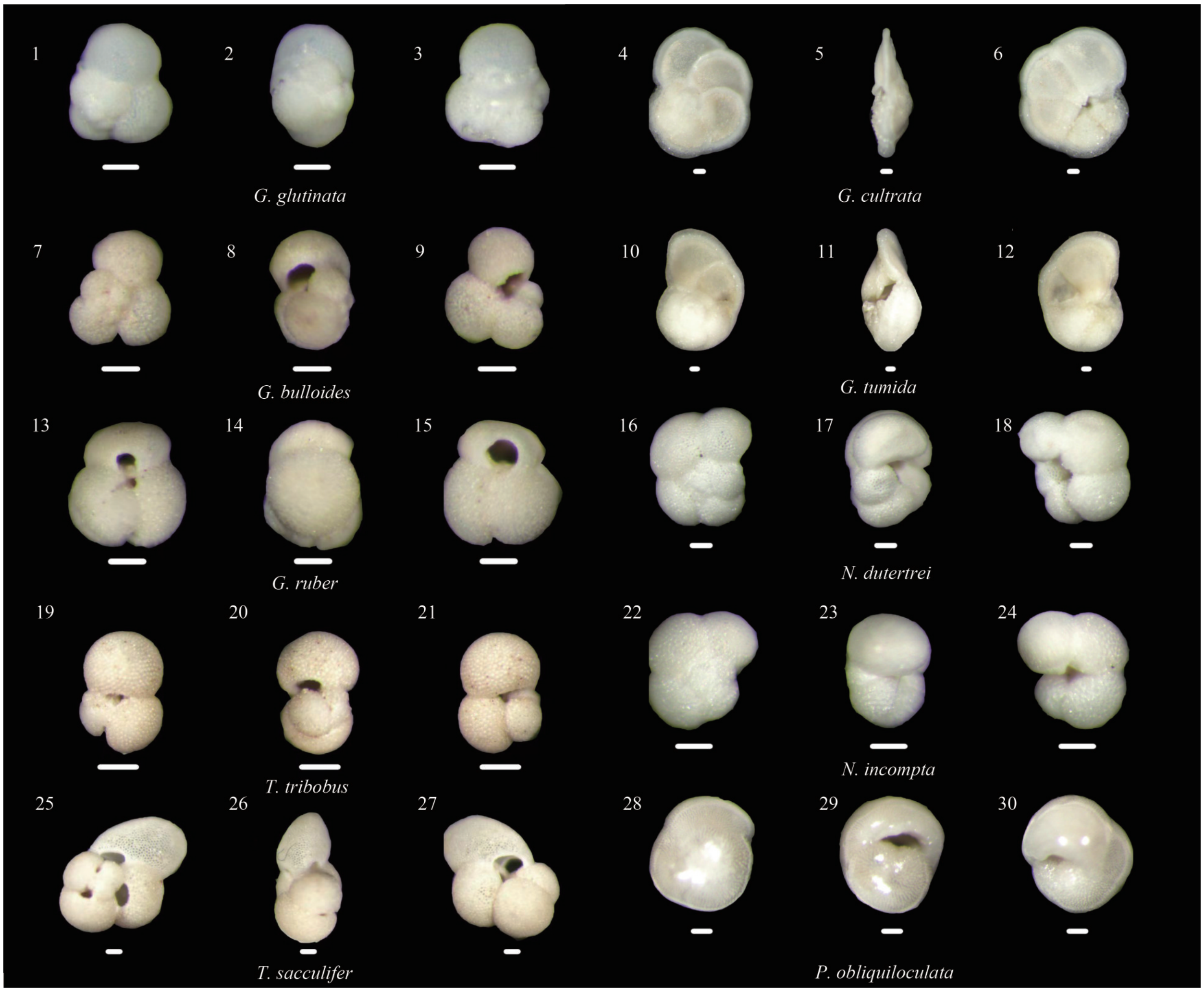

Fig.5 The stereomicroscope photographs of the main species of planktonic foraminifera in the surface sediments of the northwest Indian Ocean

All the images were taken in spiral, side, and umbilical views. Scale bars: 100 μm.

northeast monsoon, maintaining high salinity to reduce carbonate solubility.

Globorotalia tumida prefers warmer temperatures (25.3 °C average in Indian Ocean, 2.2 °C higher than *G. cultrata*) and deeper habitats (Bé and Hutson, 1977; Pflaumann and Jian, 1999; Kawahata et al., 2002; Devendra et al., 2019). It is abundant in Arabian and Somali Basins (max. 53.17%), less so in Carlsberg Ridge and northern Arabian Sea.

Pulleniatina obliquiloculata, a tropical-subtropical thermocline species (Bé and Hutson, 1977; Fairbanks et al., 1982a, 1982b; Thunell et al., 1994; Martinez et al., 1998), peaks in Somali Basin (30%), with distribution dependent on water temperature rather than depth.

Globigerinoides ruber, a widely distributed warm shallow-water soluble species (Bé and Hutson, 1977), appears at 53 stations (0–33.42% abundance), concentrated along northwest-southeast Carlsberg Ridge (often >10%, up to 30%), and is rare in Arabian and Somali Basins at 3 000–4 000-m depth (absent >4 800 m).

Neogloboquadrina dutertrei, a subtropical species favoring high primary productivity in upwelling and continental margins (Bé and Hutson, 1977; Curry et al., 1983; Ravelo et al., 1990; Cannariato and Ravelo, 1997), inhabits subsurface water/thermoclines, with >5% abundance in Carlsberg Ridge, Arabian, and Somali Basins (max. 10%), dropping >4 000-m depth.

Trilobatus trilobus, a warm current indicator in narrow warm-saline environments, shows low abundance (<3% max.) concentrated in southeast Carlsberg Ridge, absent in basin/coastal current areas.

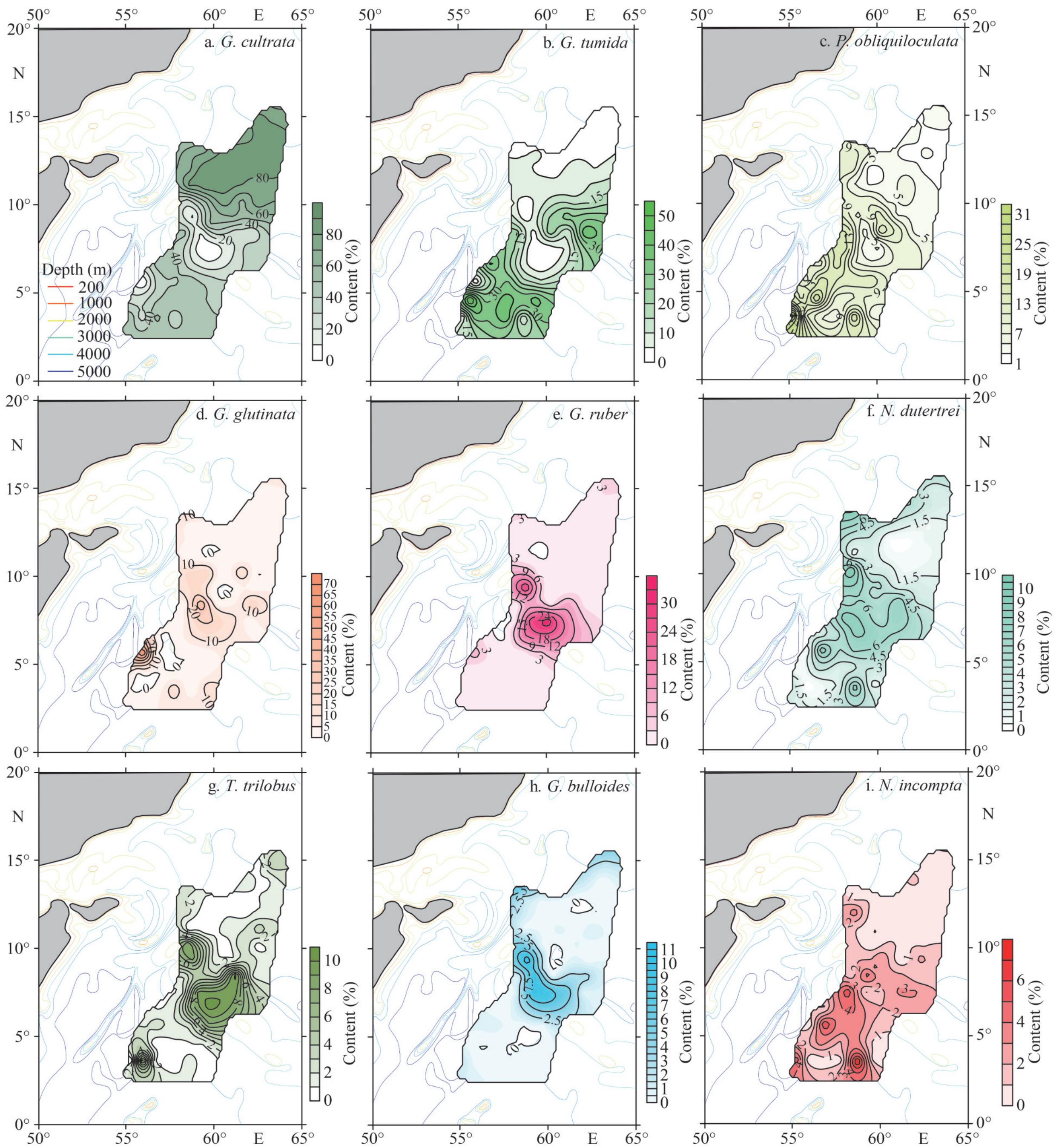

Fig.6 The percentage content of dominant planktonic foraminifera species in the study area

Globigerina bulloides, a cold-water upwelling indicator (Bé and Hutson, 1977; Cannariato and Ravelo, 1997), dominates Carlsberg Ridge, with low abundance in basins/coastal currents (slightly higher in northern Arabian Sea).

Neogloboquadrina incompta, adapted to polar-subpolar cold waters (Curry et al., 1983; Kawahata et al., 2002; Darling et al., 2006), peaks in Somali Basin (10%), rare in the northern Arabian Sea Basin.

Globigerinita glutinata peaks (70%) in the northwestern Somali Basin, coinciding with the summer upwelling zones where monsoon winds enhance nutrient fluxes (Brock et al., 1992). In contrast, *G. tumida* (5.38% in the Arabian Basin) thrives in warmer waters maintained by ASHSW during winter monsoons, as its thermal preference (25.3 °C) aligns with ASHSW temperatures (Hutson and Prell, 1980; Prell and Curry, 1981).

4.2 $CaCO_3$ content

The $CaCO_3$ content in the study area exhibits significant spatial variation, ranging from 5.91% to 89.95% with an average of 61.28%. As shown in Figs.7 and 8b, the highest values (exceeding 75%) are concentrated near the Carlsberg Ridge, where shallow water depths (below 3 700 m) and reduced carbonate dissolution create favorable preservation conditions. The Arabian Sea Basin displays moderate $CaCO_3$ contents of approximately 50%, while the Somali Basin shows the lowest values, with concentrations consistently below 25%.

This gradient reflects the combined influence of water depth, monsoon dynamics, and carbonate dissolution. The Somali Basin, with greater water depth, exceeds the carbonate compensation depth (CCD), thereby enhancing dissolution; on the other hand, the strength of the summer monsoon also plays a role, as stronger upwelling introduces nutrient-rich, acidic sub-Antarctic waters, which in turn accelerate carbonate dissolution (Wyrtki, 1973; Kroon and Ganssen, 1989; Conan et al., 2002; Böning and Bard, 2009).

5 DISCUSSION

5.1 Calcite lysocline and calcite compensation depth

It is generally accepted that the interface with $CaCO_3$ content below 10% corresponds to the CCD (Wang et al., 1995). The carbonate lysocline depth (CLD) refers to the depth at which the dissolution rate of calcium carbonate increases abruptly. The vertical distribution of each parameter in the study area is summarized in Figs.7 and 8b. The fragmentation rate remains below 15% above 3 700 m but rises sharply to over 40% at this depth, indicating a significant intensification of dissolution processes. At 3 700 m, the $CaCO_3$ content above this depth is above 75% and drops below 50% below it, further supporting the onset of intensified calcium carbonate dissolution. Within the planktonic foraminiferal abundance, the proportion of dissolution susceptible species exceeds 10% at 3 700 m but is nearly absent in deeper layers, while the proportion of dissolution resistant species increases to over 40%. Below 4 800 m, the fragmentation rate exceeds 80%. When the $CaCO_3$ content falls below 15%, the planktonic foraminifera abundance declines sharply to less than 2 000/g. Based on these observations, it can be inferred that the CLD is near 3 750 m, while the CCD is near 4 800 m. The CLD and CCD in the northwestern Indian Ocean vary regionally and are influenced by factors such as sampling density and external geological conditions. For instance, Shen et al. (2023) reported CLD of 3 900 m in the equatorial western Indian Ocean, while Banakar et al. (2010)

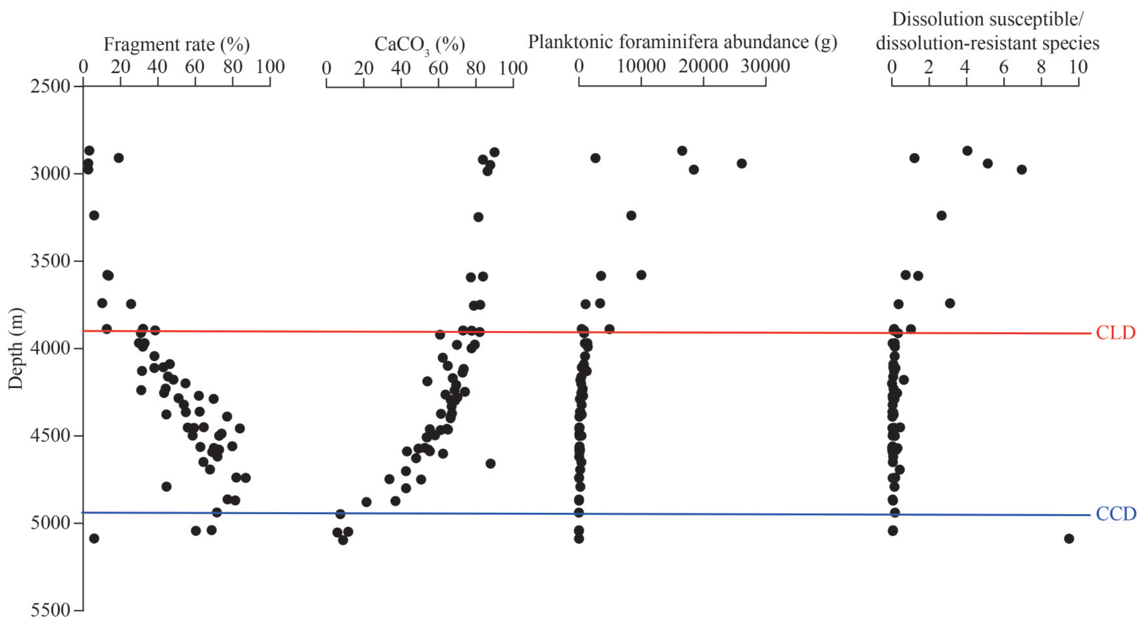

Fig.7 Vertical distribution of foraminiferal fragment rate, $CaCO_3$ content, planktonic foraminifera abundance, and dissolution susceptible/resistant species in the northern Indian Ocean, relative to the carbonate lysocline depth (CLD) (red line) and carbonate compensation depth (CCD) (blue line)

observed CLD ranging from 3 500 to 3 800 m in the east Arabian Sea. Our sampling was primarily conducted in the central region of the northwestern Indian Ocean, CLD and CCD align well with previously reported values (Bickert, 2009).

Figure 8a (benthic foraminifera percentage, BFP) and 8b ($CaCO_3$ percentage) collectively reveal the spatial differentiation of carbonate dissolution. The BFP exhibits an exponential increase with water depth (R^2=0.68), with 3 500–3 700 m being a critical threshold. In shallow regions, where the mixed layer is shallow and dissolution is weak, planktonic foraminifera are well-preserved (BFP<10%). In contrast, deep areas are leading to significant dissolution of planktonic foraminifera and a BFP rise to >30%. Correspondingly, $CaCO_3$ content decreases exponentially with increasing water depth (R^2=0.75). The Carlsberg Ridge, located above the calcite lysocline (CLD), maintains a $CaCO_3$ preservation rate >75%, whereas the Somali Basin, subjected to intense dissolution, shows $CaCO_3$<20%. Therefore, carbonate dissolution is the strongest in the Somali Basin, the weakest in the Carsberg Ridge, and the Arabian Basin in between.

5.2 Characteristic of planktonic foraminiferal assemblage and sedimentary environment

Correlation analysis of the percentage content of foraminifera can further objectively describe the relationship between the distribution of planktonic foraminifera and the marine environment of the study area (Sun et al., 2003). The R-type cluster analysis was conducted on the main foraminifera species of the study area using software SPSS. The resulting dendrogram could be divided into four groups (Fig.9), and their regional distributions were combined and divided into four assemblages (Fig.10), providing valuable insights into the characteristics of planktonic foraminiferal assemblages in the study area and their environmental indication.

In addition, we conducted a comprehensive analysis by sorting and organizing the content of the primary planktonic foraminifera and relevant background data in four distinct regions, as presented in Tables 1 and 2.

Monsoon circulation affects planktonic foraminiferal distribution by regulating conditions such as temperature, salinity, and nutrients in the ocean, shaping the characteristics of foraminiferal assemblages in different regions:

Arabian Basin (Group 1): high-salinity-low-dissolution environment dominated by northeast monsoon

The Arabian Sea Basin is influenced by the ASHSW driven by the winter northeast monsoon, with salinity of 36.2, which is significantly higher

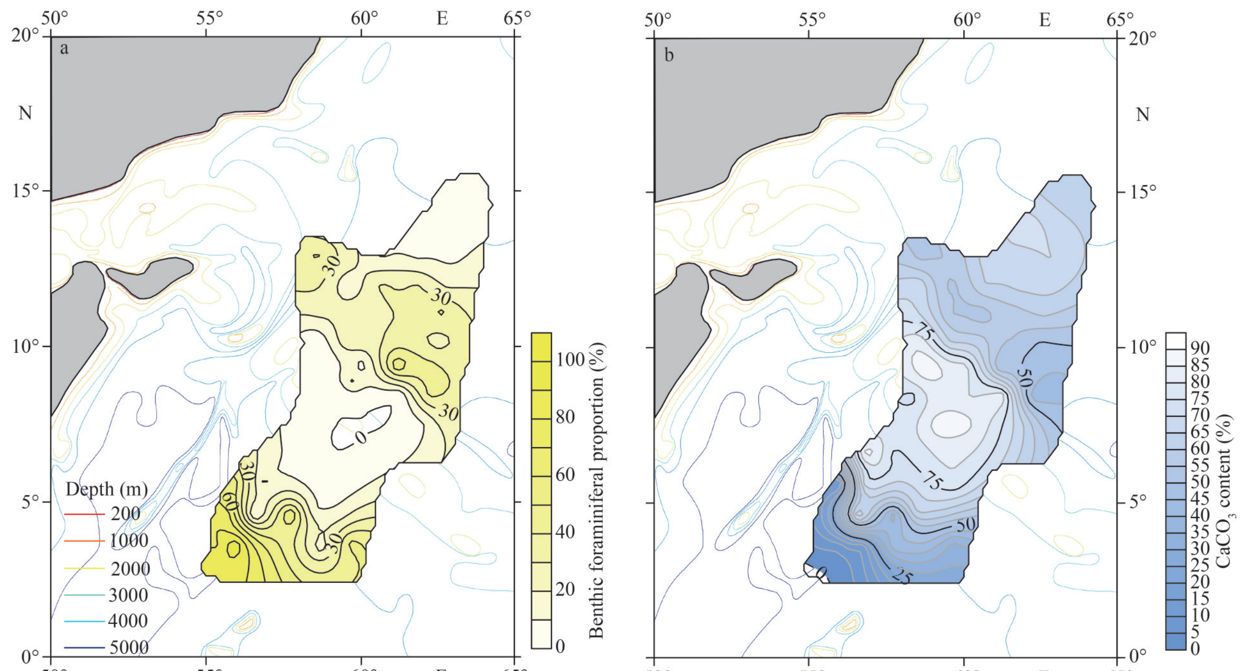

Fig.8 The spatial distribution of the benthic foraminiferal proportion (BFP) in surface sediments of the study area, showing a significant positive correlation with water depth (a) and the percentage of the $CaCO_3$ content distribution (b)

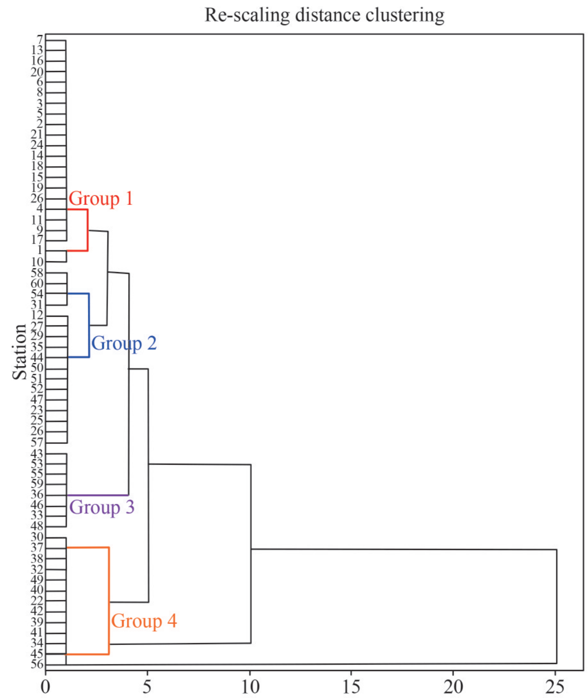

Fig.9 The dendrogram using average join of the main foraminifera species in the study area by R-type cluster analysis

than other sub-regions' (Table 2). During winter (October–April), the northeast monsoon drives the southward intrusion of ASHSW (salinity 36.2–38.2), triggering coastal upwelling through Ekman pumping (Robinson et al., 2012), which transports deep nitrate (>20 μmol/L) to the surface layer, forming a peak chlorophyll-*a* zone (1.2 mg/m^3). The chlorophyll-*a* concentration in the core area of ASHSW reached 16.26 μg/dm^3 (Fig.11). This nutrient enrichment induced by ASHSW promoted the salt-tolerant species *G. cultrata* (79.18%) to become the dominant species. Meanwhile, the monsoon-driven horizontal circulation inhibits vertical mixing, while wind stirring maintains surface nutrient concentrations, forming a positive feedback loop of "high salinity high productivity". Even during the summer southwest monsoon, Ekman pumping in the western Arabian Sea still generates upwelling, bringing nutrients without significantly reducing salinity and continuously maintaining high productivity (high chlorophyll zone shown in Fig.11), which is consistent with the role of monsoons in enhancing primary productivity, indicating that this basin is most strongly affected by winter monsoon forcing.

Carlsberg Ridge (Group 2): warm water-high productivity environment in the monsoon convergence zone

This region is characterized by alternating

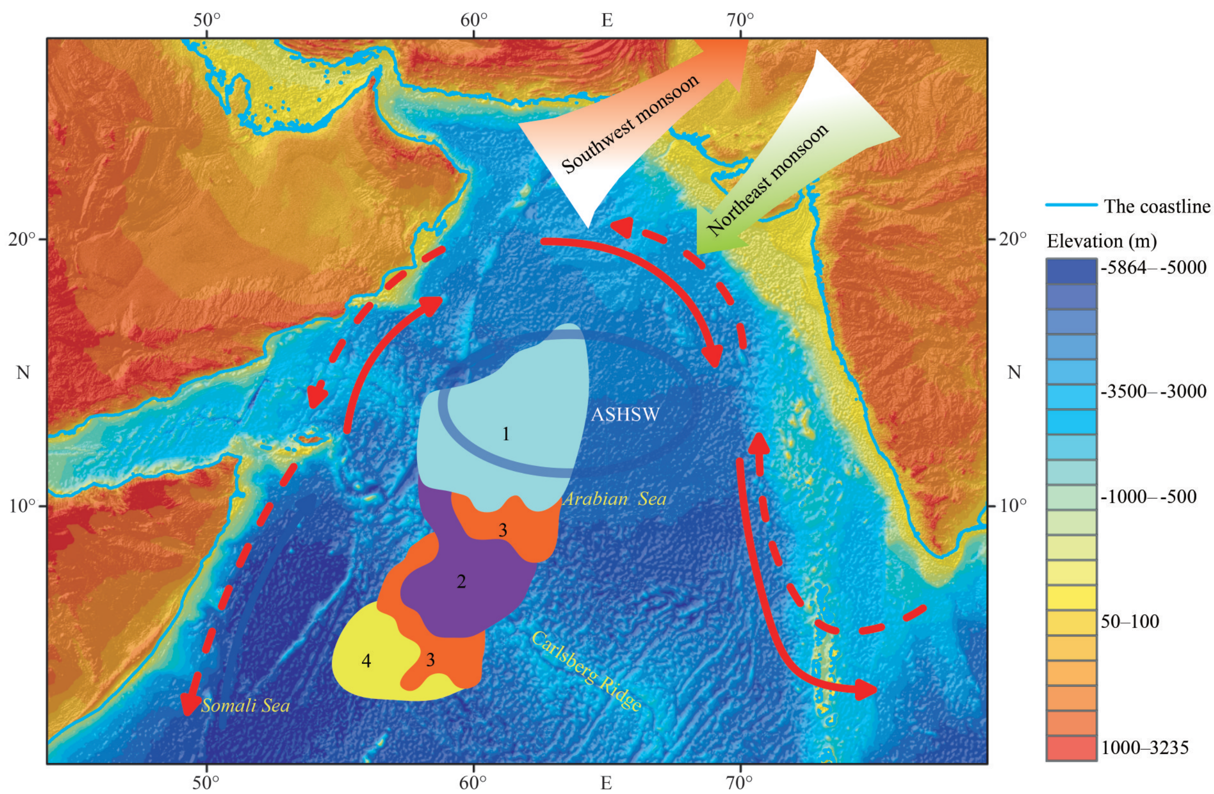

Fig.10 Four planktonic foraminifera assemblages under the influence of monsoon and sea surface circulation

Table 1 The average percentages (%) of the main genera and species of surface planktonic foraminifera in the four groups

The main species of surface planktonic foraminifera	Group 1	Group 2	Group 3	Group 4
G. bulloides	1.31	0.51	5.08	0.45
G. glutinata	2.44	5.91	17.41	0.67
G. ruber	1.34	1.09	15.07	0.92
T. trilobus	1.28	1.64	8.05	1.64
G. cultrata	79.18	45.92	17.23	41.05
G. tumida	5.38	29.08	7.66	18.58
N.dutertrei	2.68	2.35	5.90	5.92
N. incompta	0.54	1.50	2.07	4.97
P. obliquiloculata	4.08	8.24	7.55	18.90

Table 2 Marine environmental parameters of surface planktonic foraminifera subregions

Group	Environmental factor				
	Region	Ocean current	SST (°C)	SSS	Depth (m)
1	Arabian Basin	Arabian Current ASHSW	25.34	36.2	4 346
2	Carlsberg Ridge	Arabian Current—Somalia Current co-actions	26.89	35.93	4 512
3	Carlsberg Ridge flanks	Arabian Current—Somalia Current co-actions	26.89	35.54–35.93	3 820
4	Somali Basin	Somalia Current	26.86	35.54	4 261

influences of the Arabian Current and Somali Current under monsoon effects. During the summer southwest monsoon, wind-driven upwelling brings nutrient-rich deep water to the surface, increasing surface silicate concentration, which supports high biological productivity. Its temperature and salinity were greater than those of Group 1, with dominant species including *G. cultrata* (45.92%), *G. tumida* (29.08%), *P. obliquiloculata* (8.24%), and *G. glutinata* (5.91%). Among them, the abundance of *G. tumida* is significantly higher than that in Group 1, reflecting its stronger dissolution resistance and preference for warm water; the presence of *G. glutinata* and *P. obliquiloculata* may indicate monsoon-driven upwelling. In addition, the high abundance of *G. bulloides* clearly indicates ongoing upwelling in this region, and also enhances the diversity of the assemblage. Overall, the foraminiferal assemblages and oceanographic characteristics show that this region is an upwelling zone with high biological productivity.

Carlsberg Ridge Flanks (Group 3): preservation status in shallow waters and upwelling-driven productivity

The foraminiferal assemblage in the flanks of the Carlsberg Ridge dominant species included *G. glutinata* (17.41%), *G. cultrata* (17.23%), and *G. ruber* (15.07%), with *T. trilobus* (8.05%). The abundance of *G. glutinata* is significantly higher than those in the areas around, reflecting the intrusion of Subantarctic water brought by monsoon-driven upwelling, which is confirmed by elevated chlorophyll-*a* level (Fig.11). Combined with the relatively shallow water depth (compared to Groups 1 and 2) *G. ruber*, *T. trilobus*, and *G. glutinata* that contribute to the preservation, it could be determined that this region is a warm and high-productivity upwelling zone with excellent carbonate preservation.

Somali Basin (Group 4): warm water-high productivity environment under intense carbonate dissolution

During summer (May–September), offshore winds driven by the southwest monsoon trigger coastal upwelling, bringing nutrient-rich Subantarctic Mode Water and Antarctic Intermediate Water (water temperature<25 °C, salinity 35.5) to the surface (Fairbanks et al., 1982; Schott and McCreary, 2001; Schott et al., 2009), which increased surface silicate concentration (>15 μmol/L) and formed an eastward chlorophyll-*a* gradient (from 1.0 mg/m^3 in the west to 0.8 mg/m^3 in the east). The chlorophyll-*a* concentration near the upwelling core area (58.57°E, 12.03°N) was 4.67 μg/dm^3, and decreased to 3.09 μg/dm^3 in the areas more distant from coast (61.81°E, 12.88°N). Consequently, the content of *P.*

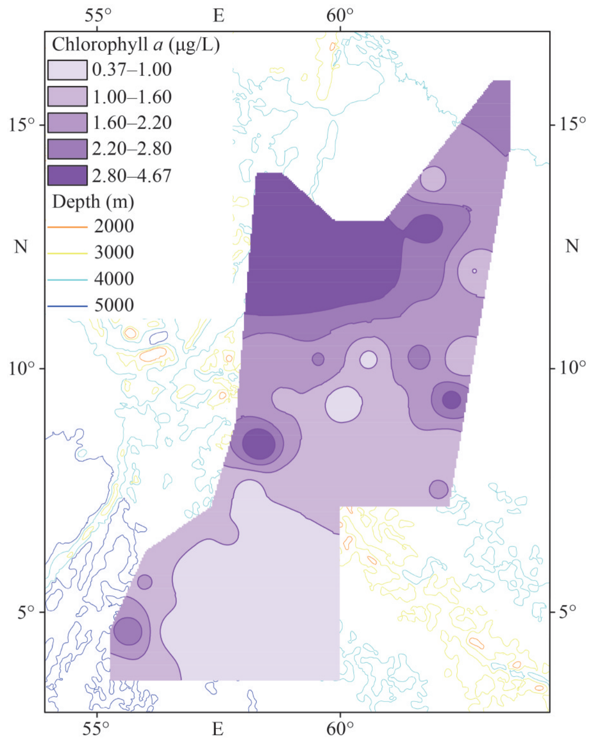

Fig.11 The chlorophyll distribution at surface water in the northwest Indian Ocean

obliquiloculata (accounting for 18.90%) increased, and *G. glutinata* reached the highest abundance (70%) in the northwest. However, due to the great water depth of the basin and the CO_2 enrichment brought by upwelling, carbonate dissolution was intensified (Böning and Bard, 2009), resulting in a fragmentation rate of 87% and carbonate content <20%, showing the characteristics of "high productivity-high dissolution-weak preservation".

The dominant species in the study region were the dissolution-resistant species *G. cultrata* (41.05%) and *G. tumida* (18.58%), and the abundances are similar to those of Group 2, reflecting the overall warm water characteristics, and these species could survive under extreme dissolution conditions. The large presence of *P. obliquiloculata* (18.90%) and *N. dutertrei* (5.92%) indicates that the upwelling signal could still be retained even under strong dissolution pressure.

6 CONCLUSION

In this study, through the identification of foraminifera in 60 surface samples of the northwest Indian Ocean and the discussion of the water depth and ocean current in the study area, the following main conclusions were drawn:

(1) The surface sediments contained 11 genera and 32 warm-water planktonic foraminiferal species, representing a typical assemblage characteristic. High abundance values were observed in relatively shallow areas located on the sea ridge.

(2) Dominant species, with an average relative abundance exceeding 5% in the planktonic foraminiferal assemblage, include *G. glutinata*, *G. cultrata*, *G. tumida*, and *P. obliquiloculata*.

(3) Four distinct planktonic foraminiferal assemblages have been identified: (a) the Arabian Basin assemblage, which reflects the influence of ASHSW and winter monsoon circulation; (b) the Carlsberg Ridge assemblage, which exhibits productivity patterns controlled by water depth; (c) the Carlsberg Ridge Flanks assemblage, which indicates monsoon-induced mixing processes; and (d) the Somali Basin assemblage, which displays clear signatures of summer monsoon-driven upwelling.

(4) Based on planktonic foraminiferal abundance, fragmentation rates, $CaCO_3$ content, and dissolution-susceptible/dissolution-resistant species, the CLD and CCD were estimated at approximately 3 700 m and 4 800 m, respectively.

7 DATA AVAILABILITY STATEMENT

Data inquiries can be directed to the corresponding author.

8 ACKNOWLEDGMENT

We thank all the crew members for their help in collecting samples and data onboard "*Xiang Yanghong 3*" during surveys. We also thank Ms. Yijun LAN (Third Institute of Oceanography, Ministry of Natural Resources) and Ms. Wenjuan SU (Third Institute of Oceanography, Ministry of Natural Resources) for their help in geochemical experiments.

References

Arumugm Y, Gupta A K, Panigrahi M K. 2014. Species diversity variations in Neogene deep-sea benthic foraminifera at ODP Hole 730A, western Arabian Sea. *Journal of Earth System Science*, **123**(7): 1671-1680, https://doi.org/10.1007/s12040-014-0495-z.

Banakar V K, Mahesh B S, Burr G et al. 2010. Climatology of the Eastern Arabian Sea during the last glacial Cycle reconstructed from paired measurement of foraminiferal $\delta^{18}O$ and Mg/Ca. *Quaternary Research*, **73**(3): 535-540, https://doi.org/10.1016/j.yqres.2010.02.002.

Banerjee R, Iyer S D. 1991. Petrography and chemistry of basalts from the Carlsberg Ridge. *Journal of the*

Geological Society of India, **38**(4): 369-386, https://doi.org/10.17491/jgsi/1991/380403.

Barber R T, Marra J, Bidigare R C et al. 2001. Primary productivity and its regulation in the Arabian Sea during 1995. *Deep Sea Research Part II*: *Topical Studies in Oceanography*, **48**(6-7): 1127-1172, https://doi.org/10.1016/S0967-0645(00)00134-X.

Bé A W H, Hutson W H. 1977. Ecology of planktonic foraminifera and biogeographic patterns of life and fossil assemblages in the Indian Ocean. *Micropaleontology*, **23**(4): 369-414, https://doi.org/10.2307/1485406.

Bé A W H, Vilks G, Lott L. 1971. Winter distribution of planktonic foraminifera between the Grand Banks and the Caribbean. *Micropaleontology*, **17**(1): 31-42, https://doi.org/10.2307/1485035.

Berger W H. 1979. Preservation of foraminifera. *In*: Lipps J H, Berger W H, Buzas M A et al. eds. Foraminiferal Ecology and Paleoecology. p.249-275, https://doi.org/10.2110/scn.79.06.

Bickert T. 2009. Carbonate compensation depth. *In*: Gornitz V ed. Encyclopedia of Paleoclimatology and Ancient Environments. Springer, Dordrecht. p.136-138, https://doi.org/10.1007/978-1-4020-4411-3_33.

Böning P, Bard E. 2009. Millennial/centennial scale thermocline ventilation changes in the Indian Ocean as reflected by aragonite preservation and geochemical variations in Arabian Sea sediments. *Geochimica et Cosmochimica Acta*, **73**(22): 6771-6788, https://doi.org/10.1016/j.gca.2009.08.028.

Boudagher-Fadel M K. 2008. Evolution and Geological Significance of Larger Benthic Foraminifera. 2nd edn. UCL Press.

Brock J C, Mcclain C R, Anderson D M et al. 1992. Southwest monsoon circulation and environments of recent planktonic foraminifera in the Northwestern Arabian Sea. *Paleoceanography*, **7**(6): 799-813, https://doi.org/10.1029/92PA01267.

Brummer G J A, Kučera M. 2022. Taxonomic review of living planktonic foraminifera. *Journal of Micropalaeontology*, **41**(1): 29-74, https://doi.org/10.5194/jm-41-29-2022, 2022.

Brummer Geert-J A, Peeters Brummer 2002 GeolSoc SpecPubl. https://doi.org/10.1144/GSL.SP.2002.195.01.26.

Cannariato K G, Ravelo A C. 1997. Pliocene-Pleistocene evolution of eastern tropical Pacific surface water circulation and thermocline depth. *Paleoceanography*, **12**(6): 805-820, https://doi.org/10.1029/97PA02514.

Cariño M C M R, Peleo-Alampay A M, Wiesner M G et al. 2023. Planktonic foraminifera fluxes and their response to the Asian monsoon: insights from the Maldives, Indian Ocean. *Frontiers in Earth Science*, **11**: 1141263, https://doi.org/10.3389/feart.2023.1141263.

Chen M T, Farrell J. 1991. Planktonic foraminifer faunal variations in the northeastern Indian Ocean: a high-resolution record of the past 800,000 years from site 758. *In*: Proceedings of the Ocean Drilling Program, Scientific Results. p.125-140.

Chen M T. 1994. Estimating thermocline from planktonic foraminifer faunal data: the development of paleoecological transfer functions for reconstructing low-latitude Pacific upper-layer conditions. *Journal of the Geological Society of China*, **37**(4): 443-474.

Chen R H, Jian Z M, Zheng Y L. 1999. Planktonic Foraminifera in the surface sediments of the southern Okinawa Trough and its geological significance. *Acta Oceanologica Sinica*, **21**(5): 78-86. (in Chinese with English abstract)

Ciarapica G. 1995. Preliminary notes on the Maldivian foraminifera from Ari and Felidu atoll (Maldives, Indian Ocean). *Revue de Paléobiologie*, **14**(2): 321-347.

Conan S M H, Ivanova E M, Brummer G J A. 2002. Quantifying carbonate dissolution and calibration of foraminiferal dissolution indices in the Somali Basin. *Marine Geology*, **182**(3-4): 325-349, https://doi.org/10.1016/S0025-3227(01)00238-9.

Curry W B, Thunell R C, Honjo S. 1983. Seasonal changes in the isotopic composition of planktonic foraminifera collected in Panama Basin sediment traps. *Earth and Planetary Science Letters*, **64**(1): 33-43, https://doi.org/10.1016/0012-821X(83)90050-X.

Dahl K A, Oppo D W. 2006. Sea surface temperature pattern reconstructions in the Arabian Sea. *Paleoceanography*, **21**(1): PA1014, https://doi.org/10.1029/2005PA001162.

Darling K F, Kucera M, Kroon D et al. 2006. A resolution for the coiling direction paradox in *Neogloboquadrina pachyderma*. *Paleoceanography*, **21**(2): PA2011, https://doi.org/10.1029/2005PA001189.

Devendra D, Xiang R, Zhong F C et al. 2019. Palaeoproductivity and associated changes in the north-eastern Indian Ocean since the last glacial: evidence from benthic foraminifera and stable isotopes. *Journal of Asian Earth Sciences*, **181**: 103913, https://doi.org/10.1016/j.jseaes.2019.103913.

Fairbanks L A, McGuire M T, Harris C J. 1982a. Nonverbal interaction of patients and therapists during psychiatric interviews. *Journal of Abnormal Psychology*, **91**(2): 109-119, https://doi.org/10.1037/0021-843X.91.2.109.

Fairbanks R G, Sverdlove M, Free R et al. 1982b. Vertical distribution and isotopic fractionation of living planktonic foraminifera from the Panama Basin. *Nature*, **298**(5877): 841-844, https://doi.org/10.1038/298841a0.

Gischler E, Hauser I, Heinrich K et al. 2003. Characterization of depositional environments in isolated carbonate platforms based on benthic foraminifera, Belize, Central America. *Palaios*, **18**(3): 236-255, https://doi.org/10.1669/0883-1351(2003)018<0236:CODEII>2.0.CO;2.

Gischler E, Hudson J H, Pisera A. 2008. Late Quaternary reef growth and sea level in the Maldives (Indian Ocean). *Marine Geology*, **250**(1-2): 104-113, https://doi.org/10.1016/j.margeo.2008.01.004.

Gupta A K, Das M, Bhaskar K. 2006. South Equatorial Current (SEC) driven changes at DSDP Site 237, Central Indian Ocean, during the Plio-Pleistocene: evidence from benthic foraminifera and stable isotopes. *Journal of Asian Earth Sciences*, **28**(4-6): 276-290, https://doi.org/10.1016/j.jseaes.2005.10.006.

Gupta A K, Thomas E. 1999. Latest Miocene-Pleistocene productivity and deep-sea ventilation in the northwestern Indian Ocean (deep sea drilling project site 219). *Paleoceanography*, **14**(1): 62-73, https://doi.org/10.1029/1998PA900006.

Gupta A K. 1997. Paleoceanographic and paleoclimatic history of the Somali Basin during the Pliocene-Pleistocene; multivariate analyses of benthic foraminifera from DSDP Site 241 (Leg 25). *Journal of Foraminiferal Research*, **27**(3): 196-208, https://doi.org/10.2113/gsjfr.27.3.196.

Hermelin J O R. 1992. Variations in the benthic foraminiferal fauna of the Arabian Sea: a response to changes in upwelling intensity? *Geological Society*, *London*, *Special Publications*, **64**: 151-166, https://doi.org/10.1144/GSL.SP.1992.064.01.10.

Hutson W H, Prell W L. 1980. A paleoecological transfer function, FI-2, for Indian Ocean planktonic foraminifera. *Journal of Paleontology*, **54**(2): 381-399.

Illing M A. 1950. The mechanical distribution of Recent Foraminifera in Bahama Banks sediments. *The Annals and Magazine of Natural History*, **3**(33): 757-761.

Jin H Y. 2004. Quaternary planktonic foraminiferal fauna and variations of the warm pool in the western equatorial Pacific. Ocean University of China, Master's Degree Thesis, Qingdao, China. (in Chinese)

Kawahata H, Nishimura A, Gagan M K. 2002. Seasonal change in foraminiferal production in the western equatorial Pacific warm pool: evidence from sediment trap experiments. *Deep Sea Research Part II*: *Topical Studies in Oceanography*, **49**(13-14): 2783-2800, https://doi.org/10.1016/S0967-0645(02)00058-9.

Kennett J P. 1983. Neogene Planktonic Foraminifera: a Phylogenetic Atlas. Hutchinson Ross Publishing Company.

Kroon D, Ganssen G. 1989. Northern Indian Ocean upwelling cells and the stable isotopes composition of living planktonic foraminifers. *Deep Sea Research Part A*: *Oceanographic Research Papers*, **36**(8): 1219-1236, https://doi.org/10.1016/0198-0149(89)90102-7.

Kroon D, Steens T, Troelstra S R. 1991. Onset of monsoonal related upwelling in the western Arabian sea as revealed by planktonic foraminifers. *In*: Proceedings of the Ocean Drilling Program. p.257-263.

Le J N, Shackleton N J. 1992. Carbonate dissolution fluctuations in the western equatorial Pacific during the late Quaternary. *Paleoceanography*, **7**(1): 21-42, https://doi.org/10.1029/91PA02854.

Liu S Q, Chen W L, Zhang M H et al. 2022. Distribution of planktonic foraminifera in surface sediments and its environmental implication in the Zhongsha waters, South China Sea. *Marine Geology Frontiers*, **38**(9): 13-25, https://doi.org/10.16028/j.1009-2722.2021.312. (in Chinese with English abstract)

Martinez J I, Taylor L, De Deckker P et al. 1998. Planktonic foraminifera from the eastern Indian Ocean: distribution and ecology in relation to the Western Pacific Warm Pool (WPWP). *Marine Micropaleontology*, **34**(3-4): 121-151, https://doi.org/10.1016/S0377-8398(97)00045-5.

Pandey D K, Clift P D, Kulhanek D K et al. 2015. Arabian sea monsoon: deep sea drilling in the Arabian Sea: constraining tectonic-monsoon interactions in South Asia. IODP.

Peng S Q, Qian Y K, Lumpkin R et al. 2015. Characteristics of the near-surface currents in the Indian Ocean as deduced from satellite-traced surface drifters. Part I: pseudo-eulerian statistics. *Journal of Physical Oceanography*, **45**(2): 441-458, https://doi.org/10.1175/JPO-D-14-0050.1.

Pflaumann U, Jian Z M. 1999. Modern distribution patterns of planktonic foraminifera in the South China Sea and western Pacific: a new transfer technique to estimate regional sea surface temperatures. *Marine Geology*, **156**(1-4): 41-83, https://doi.org/10.1016/S0025-3227(98)00173-X.

Prasad T G, Ikeda M, Kumar S P. 2001. Seasonal spreading of the Persian Gulf Water mass in the Arabian Sea. *Journal of Geophysical Research*: *Oceans*, **106**(C8): 17059-17071, https://doi.org/10.1029/2000JC000480.

Prell W L, Curry W B. 1981. Faunal and isotopic indices of monsoonal upwelling: western Arabian Sea. *Oceanologica Acta*, **4**(1): 91-98.

Quadfasel D R, Schott F. 1982. Water-mass distributions at intermediate layers off the Somali Coast during the onset of the southwest monsoon, 1979. *Journal of Physical Oceanography*, **12**(12): 1358-1372, https://doi.org/10.1175/1520-0485(1982)012<1358:WMDAIL>2,0,CO;2.

Rai A K, Srinivasan M S. 1994. Pleistocene oceanographic changes indicated by deep sea benthic foraminifera in the northern Indian Ocean. *Proceedings of the Indian Academy of Sciences-Earth and Planetary Sciences*, **103**(4): 499-517, https://doi.org/10.1007/BF02839293.

Rao R R, Sivakumar R. 1998. Observed seasonal variability of heat content in the upper layers of the tropical Indian Ocean from a new global ocean temperature climatology. *Deep Sea Research Part I*: *Oceanographic Research Papers*, **45**(1): 67-89, https://doi.org/10.1016/S0967-0637(97)00066-6.

Ravelo A C, Fairbanks R G, Philander S G H. 1990. Reconstructing tropical Atlantic hydrography using planktontic foraminifera and an ocean model. *Paleoceanography*, **5**(3): 409-431, https://doi.org/10.1029/PA005i003p00409.

Ravichandran M, Gupta A K, Mohan K et al. 2021. Indian monsoon wind variability since ~11 kyr in the northwestern and northeastern Arabian Sea. *Journal of Asian Earth Sciences*, **218**: 104882, https://doi.org/10.1016/j.jseaes.2021.104882.

Ray D, Kamesh Raju K A, Baker E T et al. 2012. Hydrothermal plumes over the Carlsberg Ridge, Indian Ocean. *Geochemistry*, *Geophysics*, *Geosystems*, **13**(1): Q01009, https://doi.org/10.1029/2011GC003888.

Rippert N, Baumann K H, Pätzold J. 2015. Thermocline fluctuations in the western tropical Indian Ocean during the past 35 ka. *Journal of Quaternary Science*, **30**(3): 201-210, https://doi.org/10.1002/jqs.2767.

Robinson M M, Dowsett H J, Stoll D K. 2012. Indian Ocean planktic foraminiferal distribution and sea surface temperature estimates of the warm mid-Piacenzian with implications for the instability of monsoon-related upwelling and the Indian Ocean dipole. *In*: American Geophysical Union, Fall Meeting 2012. American Geophysical Union.

Schott F A, McCreary Jr J P. 2001. The monsoon circulation of the Indian Ocean. *Progress in Oceanography*, **51**(1): 1-123, https://doi.org/10.1016/S0079-6611(01)00083-0.

Schott F A, Xie S P, Mccreary Jr J P. 2009. Indian Ocean circulation and climate variability. *Reviews of Geophysics*, **47**(1): RG1002, https://doi.org/10.1029/2007RG000245.

Shen W, Qiao S Q, Sun R T et al. 2023. Distribution pattern of planktonic and benthic foraminifera in surface sediments near the equatorial western Indian Ocean and its indications of paleo-environment and productivity. *Journal of Asian Earth Sciences*, **250**: 105635, https://doi.org/10.1016/j.jseaes.2023.105635.

Spezzaferri S, Kucera M, Pearson P N et al. 2015. Fossil and genetic evidence for the polyphyletic nature of the planktonic foraminifera "*Globigerinoides*", and description of the new genus *Trilobatus*. *PLoS One*, **10**(5): e0128108, https://doi.org/10.1371/journal.pone.0128108.

Sun R T, Li T G, Cao Q Y et al. 2003. Planktonic foraminifera distributions in surface sediments of the northern Okinawa Trough and their marine environment interpretation. *Oceanologia et Limnologia Sinica*, **34**(5): 511-518.

Thunell R, Anderson D, Gellar D et al. 1994. Sea-surface temperature estimates for the tropical western Pacific during the last glaciation and their implications for the Pacific warm pool. *Quaternary Research*, **41**(3): 255-264, https://doi.org/10.1006/qres.1994.1029.

Wang P X, Zhang J J, Zhao Q H et al. 1988a. Foraminifera and ostracoda in sediments of the East China Sea. China Ocean Press, Beijing. (in Chinese)

Wang P X, Zhang J J, Zhao Q H. 1988b. Foraminifera and Ostracoda in Bottom Sediments of the East China Sea. Ocean Press, Beijing. (in Chinese)

Wang P X. Wang L J, Bian Y Het al. 1995. Late Quaternary Paleoceanography of the South China Sea: surface circulation and carbonate cycles. *Marine Geology*, **127**(1-4): 145-165, https://doi.org/10.1016/0025-3227(95)00008-M.

Wyrtki K. 1973. Physical oceanography of the Indian Ocean. *In*: Zeitzschel B, Gerlach S A eds. The Biology of the Indian Ocean. Springer, Berlin. p.18-36, https://doi.org/10.1007/978-3-642-65468-8_3.

You Y Z. 1997. Seasonal variations of thermocline circulation and ventilation in the Indian Ocean. *Journal of Geophysical Research*: *Oceans*, **102**(C5): 10391-10422, https://doi.org/10.1029/96JC03600.